

## Article

# Aerogel-Like Material Based on PEGylated Hyperbranched Polymethylethoxysiloxane

Kirill Borisov <sup>1,2</sup>, Alexandra Kalinina <sup>1,2</sup> , Aleksandra Bystrova <sup>1,2</sup> and Aziz Muzafarov <sup>1,2,\*</sup> 

<sup>1</sup> A.N. Nesmeyanov Institute of Organoelement Compounds, Russian Academy of Sciences, 119334 Moscow, Russia; borisov@ispm.ru (K.B.)

<sup>2</sup> Enikolopov Institute of Synthetic Polymeric Materials, Russian Academy of Sciences, 117393 Moscow, Russia

\* Correspondence: aziz@ispm.ru

**Abstract:** Aerogels are a class of materials that have gained increasing attention over the past several decades due to their exceptional physical and chemical properties. These materials are highly porous, with a low density and high surface area, allowing for applications such as insulation, catalysis, and energy storage. However, traditional aerogels, such as pure silica aerogels, suffer from brittleness and fragility, which limit their usefulness in many applications. Herein, we have addressed this problem by using organosilicon compounds, namely polymethylsilsesquioxane derivatives, for the synthesis of aerogel-like materials. Specifically, we have developed a novel approach involving surfactant-free synthesis of microcapsules from partially PEGylated hyperbranched polymethylethoxysiloxane. Due to the highly diphilic nature of these compounds, they readily concentrate at the oil/water interface in aqueous emulsions encapsulating oil droplets. During the subsequent condensation, the organosilicon precursor is consumed for hexane encapsulation (yielding hollow microcapsules) followed by the formation of a continuous condensed phase. Concurrently, methyl groups ensure the hydrophobicity of the resulting materials, which eliminates the need of using additional reagents for their hydrophobization.

**Keywords:** polymethylsilsesquioxanes; hyperbranched polymers; nanogels; aerogels; microencapsulation; surfactant-free emulsions; hydrophilic–lipophilic balance



**Citation:** Borisov, K.; Kalinina, A.; Bystrova, A.; Muzafarov, A. Aerogel-Like Material Based on PEGylated Hyperbranched Polymethylethoxysiloxane. *Polymers* **2023**, *15*, 4012. <https://doi.org/10.3390/polym15194012>

Academic Editor: Iolanda De Marco

Received: 28 August 2023

Revised: 25 September 2023

Accepted: 25 September 2023

Published: 7 October 2023



**Copyright:** © 2023 by the authors. Licensee MDPI, Basel, Switzerland. This article is an open access article distributed under the terms and conditions of the Creative Commons Attribution (CC BY) license (<https://creativecommons.org/licenses/by/4.0/>).

## 1. Introduction

Aerogels hold immense potential for a wide range of applications across various domains. The vast potential for further development and refinement of aerogel-based materials makes them a subject of continued interest and exploration. They have found utility in areas such as sound insulation [1,2], thermal insulation [3,4], optical materials [5,6], as well as food industry [7] and numerous other fields. Among the diverse spectrum of materials capable of forming aerogel frameworks, such as carbon nanotubes [8–10], cellulose [11,12], polymer nanofibers [13], and natural substances [14–17], silica aerogels are among the most renowned. These materials were originally conceptualized by Kistler in 1931, and his groundbreaking work introduced the pioneering method of supercritical drying [18]. This method, which is now widely employed, facilitates the creation of aerogels with exceptionally low density and high porosity.

Silica and organosilicon aerogels have become a focal point of extensive research efforts, boasting a rich literature spanning multiple studies [19–27]. These studies explore a wide array of methodologies for their synthesis. Precursors employed in the fabrication of silicon–organic aerogels encompass a diverse range of substances. These include sodium silicate [19,20], methyltriethoxysilane [21], methyltrimethoxysilane [22–24], tetraethoxysilane [25], tetramethoxysilane [26], perfluoroalkylsilane [27], and many other silanes, often in combination with one another.

A crucial stage in the fabrication of aerogels is the drying process, as it plays a fundamental role in preserving the gel's structure and, consequently, its physical and mechanical

properties, as well as its porosity. There are three primary drying methods employed for their production.

The first of these methods is supercritical drying, which, while costly, proves highly effective. This technique is executed under elevated temperature and pressure conditions, inducing the transition of the liquid into a supercritical state. This transformation effectively negates the impact of capillary forces that might otherwise cause gel collapse [28]. Supercritical drying finds extensive use in the production of organosilicon aerogels [18,23,26].

The second method involves drying under ambient conditions [29–31]. This type of drying is notably straightforward to implement since it does not necessitate expensive or complex processes. However, it does impose limitations on the chemical composition of the gels. This is because, in cases where the gel's pore surfaces are hydrophilic, the removal of water can lead to significant gel shrinkage, negatively impacting its properties. To mitigate this effect, hydrophobic silanes like trimethylchlorosilane, dimethyldichlorosilane, trimethylethoxysilane, methyltrimethoxysilane, and certain other silanes could be employed.

The third method is the freeze-drying of gels [20,32,33]. To execute this method, the liquid within the gel is frozen and then subjected to sublimation under vacuum conditions. This technique is more cost-effective compared to supercritical drying and can also prevent gel shrinkage. However, it does come with its limitations. The solvent's crystallization during freezing can potentially compromise the integrity of the gel structure, leading to the formation of cracks.

An approach method for achieving a highly porous structure involves assembling specific micro-objects as building blocks, resulting in a hierarchically organized structure that combines high porosity with mechanical strength surpassing that of conventional aerogels. Güler et al. [34] have successfully applied this approach to create high-capacity adsorbents, and other researchers [35,36] have explored its potential in thermal insulation materials. Nevertheless, instances of this approach remain limited in the literature.

The basis of the current study is to further development of the concept of creating hollow particles using hyperbranched polyethoxysiloxane (PEOS) as a multifunctional inorganic matrix of dense globular shape [37–39]. Poly (ethylene glycol) derivatives of PEOS exhibit enhanced surface activity at the water–oil interface, enabling the production of nanoscale hollow silica particles [40,41]. Here, aerogel-like materials were prepared based on PEGylated hyperbranched polymethylethoxysiloxanes (PMEOS) in oil-in-water emulsions. The evolution of the PEGylated hyperbranched PMEOS in water involves polycyclization with the formation of a nanogel structure [42,43] and further assembly of the nanogel particles on the hexane–water phase boundary. During gelation, nanogel particles form crosslinked layers around hexane droplets, encapsulating them (forming hollow microcapsules) and a continuous condensed phase that binds the emerging microcapsules. The methyl groups confer hydrophobicity to the resulting materials, obviating the need for additional reagents and processes to make them hydrophobic.

## 2. Materials and Methods

### 2.1. Materials

Methyltriethoxysilane (99% Reachem, Moscow, Russia) was distilled under argon prior to use. Acetic acid (99% Component-Reaktiv, Moscow, Russia), and ethanol were dried by prolonged boiling, followed by distillation over  $P_2O_5$  under argon. Sodium hydroxide (99% Component-Reaktiv, Moscow, Russia), aqueous solution of ammonia (25%, SIGMATEK, Khimki, Russia), poly(ethylene glycol) monomethyl ether (average molecular weight 350, ABCR, Karlsruhe, Germany), and hexane (99% Component-Reaktiv, Moscow, Russia) were used as received. Deionized water was used for all experiments.

Synthesis of hyperbranched polymethylethoxysiloxane (PMEOS). The synthesis was conducted using the methodology first described in [44]. A total of 267.5 g (1.5 moles) of methyltriethoxysilane (MTES) was dissolved in toluene to obtain 50% solution. The dissolution process was carried out at a temperature of  $T = 20 \pm 5$  °C for 5 min. An amount

of 60 g (1.5 moles) of sodium hydroxide was added to the prepared solution. The mixture was vigorously stirred under an argon atmosphere until the sodium hydroxide particles disappeared. The resulting solution was diluted with toluene to a 25% concentration, and then 90 g (1.5 moles) of acetic acid were added dropwise. The mixture was stirred at a temperature of  $T = 20 \pm 5 \text{ }^\circ\text{C}$  for 3 h. The prepared mixture was filtered using a Schott filter, and the solvent was removed using a rotary evaporator and a vacuum pump. The yield of the product was 136.1 g (87%).

PEGylation of hyperbranched PMEOS with a degree of ethoxy group substitution of 5, 10, 20 mol% (PMEOS-PEG-5, 10, 20) was conducted as follows: PMEOS was mixed with the calculated amount of PEG and stirred on an oil bath at a temperature of  $135 \text{ }^\circ\text{C}$  for 6 h with the distillation of the generated ethanol. Subsequently, residual ethanol was removed by vacuum treatment (see Table 1 for loadings and yield).

**Table 1.** Loadings for the synthesis of PMEOS-PEG-5, 10 and 20.

Product	Ethoxy Group Substitution (mol%)	Mass of PMEOS (g)	Mass of PEG (g)	Yield (%)—(g)
PMEOS-PEG-5	5	40	4.5	(99%)—43.7
PMEOS-PEG-10	10	40	9	(99%)—47.5
PMEOS-PEG-20	20	40	18	(99%)—55.2

PEGylation of hyperbranched PMEOS with a degree of ethoxy group substitution of 10 mol% (PMEOS-PEG-10) was conducted as follows: 40 g of PMEOS was mixed with 9 g of PEG and stirred on an oil bath at a temperature of  $135 \text{ }^\circ\text{C}$  for 6 h with the distillation of the generated ethanol. Subsequently, residual ethanol was removed by vacuum treatment. The yield of the product was 47.5 g (99%).

PEGylation of hyperbranched PMEOS with a degree of ethoxy group substitution of 5 mol% (PMEOS-PEG-5) was conducted as follows: 40 g of PMEOS was mixed with 4.5 g of PEG and stirred on an oil bath at a temperature of  $135 \text{ }^\circ\text{C}$  for 6 h with the distillation of the generated ethanol. Subsequently, residual ethanol was removed by vacuum treatment. The yield of the product was 43.7 g (99%).

Preparation of Aerogel. In 50 g of water, 1, 2, or 3 g of PMEOS-PEG was dispersed in 50 g of water. An amount of 1 g of hexane was added to this emulsion, and the mixture was stirred for 5 min at 700 rpm. Then, 2.5 g of ammonia was added, and stirring continued until gelation. The obtained gel was aged for a week and then subjected to freeze-drying for 48 h at a pressure of 0.08 Torr.

## 2.2. Methods

**GPC Analysis.** Gel-permeation chromatography (GPC) was performed on a chromatographic system consisting of a STAIER series II high-pressure pump (Aquila, Nakhodka, Russia), a RIDK 102 refractometric detector (Czech Republic), and a JETSTREAM 2 PLUS column thermostat (KNAUER, Berlin, Germany). The temperature was controlled at  $40 \text{ }^\circ\text{C}$  ( $\pm 0.1 \text{ }^\circ\text{C}$ ). Tetrahydrofuran was used as the eluent, the flow rate was 1.0 mL/min. A  $300 \times 7.8 \text{ mm}$  column filled with Phenogel sorbent (Phenomenex, Torrance, CA, USA), particle size of  $5 \text{ }\mu\text{m}$ , and a pore size of  $103 \text{ \AA}$  were used (passport separation range—up to 75,000 D). Recording and processing of data was carried out using UniChrom 4.7 software (Minsk, Belarus).

**$^1\text{H}$  NMR Spectroscopy.**  $^1\text{H}$  NMR spectra were acquired using a Bruker WP250 SY spectrometer with  $\text{CDCl}_3$  as the solvent.

**IR spectroscopy.** IR spectra were recorded on a Bruker Tensor 27 spectrometer in the ATR mode of 4 scans for each wave number in the range of  $550\text{--}4000 \text{ cm}^{-1}$ .

**Interfacial Tension Measurement.** The interfacial tension (IFT) between the water and oil phases was determined using a Krüss spinning drop tensiometer at a temperature of  $25 \text{ }^\circ\text{C}$ .

**Contact Angle Measurement.** Contact angle measurements were performed using the Krüss easy drop instrument.

**Scanning Electron Microscopy.** Scanning electron microscopy (SEM) was conducted using a JCM-6000 PLUS microscope equipped with an energy-dispersive spectrometer, operating at accelerating voltages ranging from 5 to 15 kV.

**Transmission Electron Microscopy.** Transmission electron microscopy (TEM) was performed using a JEM-2100F microscope.

**Specific Surface Area Measurement.** Nitrogen adsorption was measured using the dynamic adsorption–desorption method on a “Sorbi–MS” instrument (META, Russia) with helium as the carrier gas. The specific surface area of the materials was evaluated using the four-point BET method within a range of relative pressure ( $p/p_0$ ) of 0.06 to 0.2.

**Mechanical Properties.** Cylinder-shaped samples with dimensions of 35 mm × 24 mm (height × diameter) were loaded into a Mecmesin MultiTest 2.5-i instrument and subjected to uniaxial compression at 25 °C and a constant deformation rate of 1 mm/min.

**Oil Absorption Capacity Measurement.** An amount of 0.2 g of the sample was mixed with 10 g of sunflower oil, stirred for 30 min, and subsequently subjected to centrifugation at 3000 rpm for 15 min. After centrifugation, the oil was decanted, and the sediment was then weighed.

### 3. Results and Discussion

#### *Synthesis and Properties of PMEOS-PEG*

According to the scheme depicted in Figure 1, three samples of PMEOS-PEG were synthesized, containing 5, 10, and 20 mol% ethylene glycol substituents.  $^1\text{H}$  NMR data (Figure 2a) indicated that the quantity of substituted ethoxy groups is in good agreement with theoretical calculations, measuring 4.8, 10.4, and 19.2 mol%, correspondingly. Additionally, as demonstrated by GPC results (Figure 2b), all three PMEOS-PEG samples exhibit nearly identical molecular weight distributions.

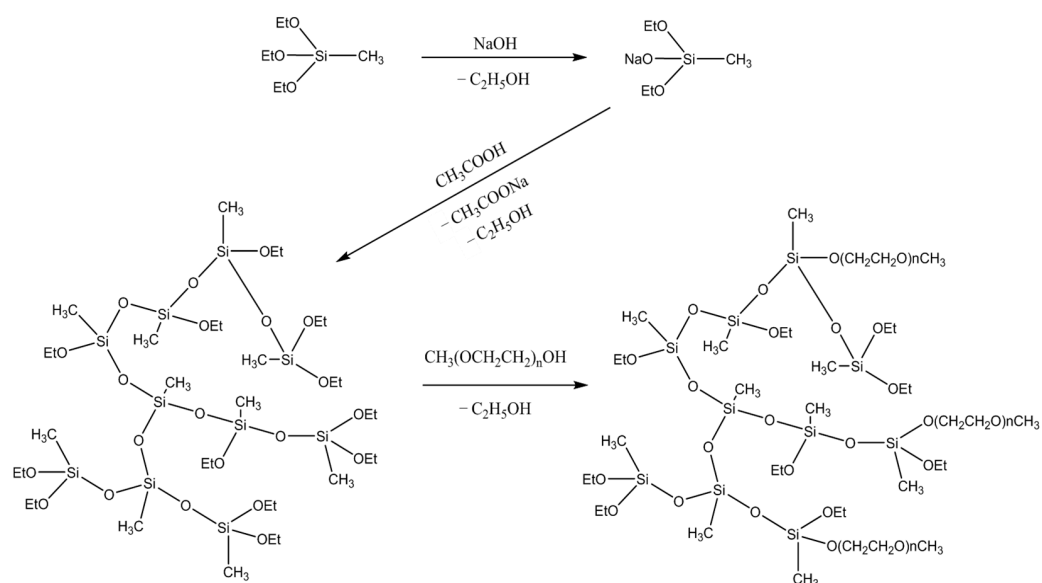


**Figure 1.** Synthesis of PMEOS-PEG.



Hence, we hypothesized that these PMEOS-PEG condensation conditions would facilitate the production of hollow particles of minimal dimensions.

**Table 3.** IFT between PMEOS-PEG dispersion in water and hexane.

Sample	Concentration of PMEOS-PEG in Water (%)	IFT (mN/m) <sup>1</sup>
PMEOS-PEG-5	0.1	12.5
PMEOS-PEG-5	1	10
PMEOS-PEG-5	5	-
PMEOS-PEG-10	0.1	10.2
PMEOS-PEG-10	1	7
PMEOS-PEG-10	5	-
PMEOS-PEG-20	0.1	6.6
PMEOS-PEG-20	1	4.9
PMEOS-PEG-20	5	1.9

<sup>1</sup> Due to the fact that the interfacial tension evaluation method is optical, investigating the surface activity of PMEOS-PEG-5 and PMEOS-PEG-10 at their 5% concentration in water was not feasible due to the excessive turbidity of these mixtures.

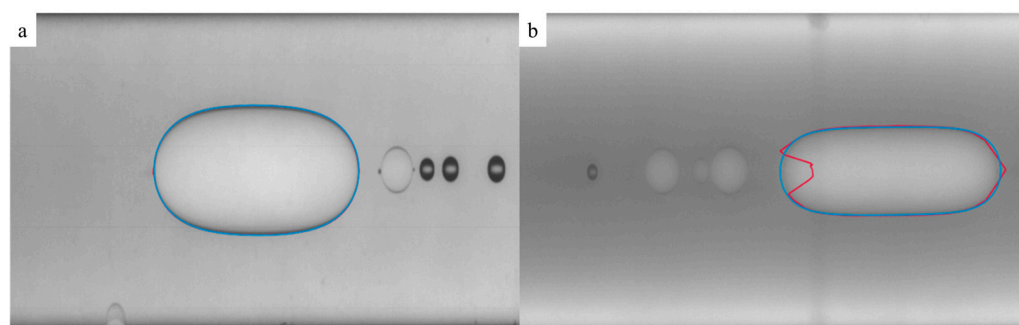


**Figure 3.** Hexane droplet in water in the presence of PMEOS-PEG-20 (PMEOS-PEG-20 content in water—0.1% (a) and 5% (b)).

To produce aerogels, three PMEOS-PEG-20 to hexane mass ratios were employed: 1:1, 2:1, and 3:1 (designated as samples No. 1, 2, and 3, respectively), and the gelation of the prepared emulsions occurred after 11, 7, and 3 h, respectively. After aging for a week and freeze-drying for 48 h, a soft, elastic, yet crumbling material was obtained (Figure 4b). SEM and TEM images (Figure 4c,d) demonstrate that the hollow particles within the aerogel are polydisperse and range in size from 100 nm to 1.5  $\mu\text{m}$ . The masses after freeze-drying were 0.79, 1.63, and 2.54 g, and the densities were 0.038, 0.04, and 0.059  $\text{g}/\text{cm}^3$  for samples 1, 2, and 3, respectively. The contact angle values of water droplets on the surface of these materials were measured to be  $120 \pm 7^\circ$ . These contact angle values are influenced by the presence of methyl groups within the gel composition. However, the presence of residual hydroxyl and ethoxy groups (Figure 5c) hinders the attainment of materials with greater hydrophobicity.

After annealing for 2 h at 200  $^\circ\text{C}$ , the aerogels lost a significant amount of their mass (Table 4), along with a decrease in their density. The reduction in these parameters indicates a substantial amount of unreacted ethoxy groups presented in the samples prior to annealing, which is confirmed by the decrease in the intensity of peaks around 2900  $\text{cm}^{-1}$  corresponding to the vibrations of methyl components of the ethoxy groups (Figure 5c), and a small amount of hydroxyl groups (3350–3600  $\text{cm}^{-1}$ ) (Figure 5d). It is important to emphasize here that such a significant loss of mass was accompanied with only 11.5% volumetric shrinkage (calculated from the dimensions of the samples), as the porous structure is established during the hexane encapsulation process. This fact is further

confirmed by measurement of average specific surface area which increased after annealing by more than 100 times (see Table 4) from  $1.25 \text{ m}^2/\text{g}$  for all samples before annealing.

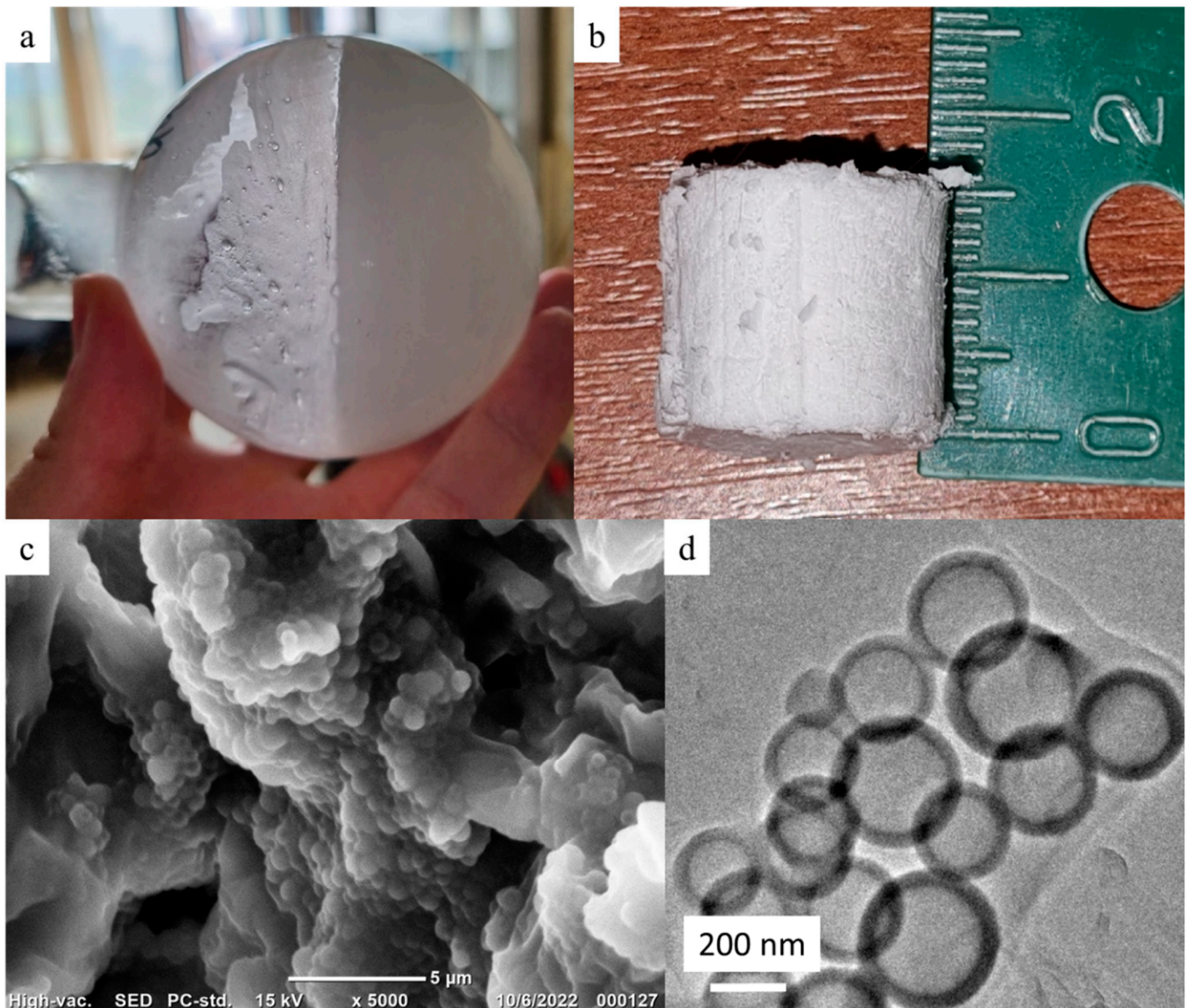


**Figure 4.** Gel in the flask (a), gel after freeze-drying (b), SEM image of Sample 2 after annealing (c), TEM image of Sample 2 after annealing (d).

**Table 4.** Properties of obtained aerogels.

Sample	PMEOS-PEG-20:Hexane	Before Annealing			After Annealing <sup>1</sup>		
		Density, $\text{g}/\text{cm}^3$	Contact Angle, $^\circ$	Mass Loss, %	Density, $\text{g}/\text{cm}^3$	Contact Angle, $^\circ$	Specific Surface Area (BET), $\text{m}^2/\text{g}$
1	1:1	0.038	$120 \pm 7$	59	0.015	$140 \pm 2$	$122 \pm 7$
2	2:1	0.040	$120 \pm 7$	53	0.021	$140 \pm 2$	$337 \pm 17$
3	3:1	0.059	$120 \pm 7$	55	0.026	$140 \pm 2$	$244 \pm 12$

<sup>1</sup> Samples were annealed at  $200 \text{ }^\circ\text{C}$  for 2 h.

Upon the removal of residual ethoxy and hydroxyl groups, the contact angle reaches values of  $140 \pm 2^\circ$  (Table 3, Figure 6) for annealed samples. These elevated contact angle values contribute to the aerogels' excellent hydrophobicity, effectively averting the absorp-

tion of moisture from the surrounding environment and, consequently, preserving their physical and mechanical properties.

To determine the oil absorption capacity of the aerogel samples, we investigated their sorption properties with sunflower oil. The sorption results were as follows: 10.9 g of oil per 1 g of gel for sample 1, 13.1 g of oil per 1 g of gel for sample 2, and 11.4 g of oil per 1 g of gel for sample 3. These values align with the variations in specific surface area among the samples.

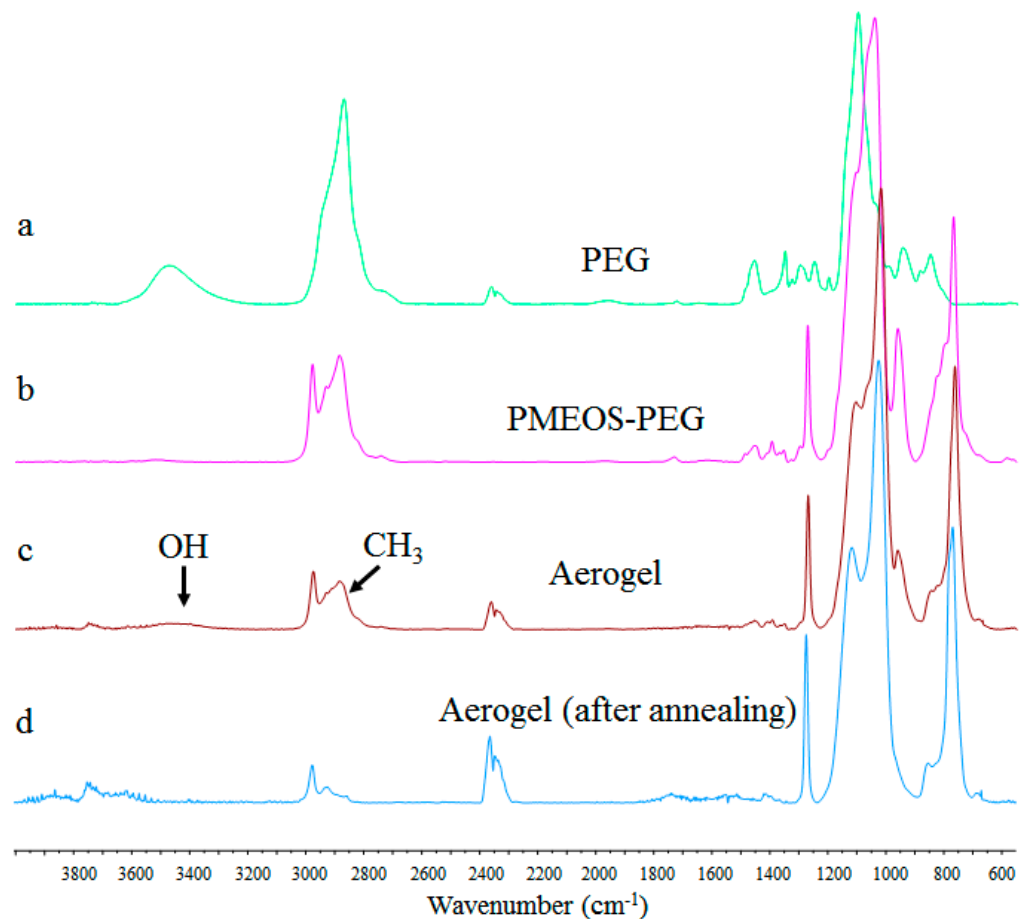


**Figure 5.** IR spectra of PEG (a), PMEOS-PEG-20 (b), aerogel sample after freeze-drying (c), aerogel sample after annealing at 200 °C for 2 h (d).

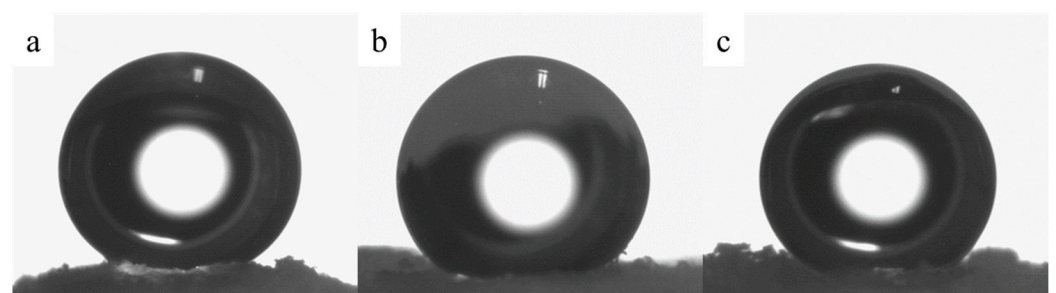


**Figure 6.** Water droplet on the surface of aerogel samples 1 (a), 2 (b), and 3 (c).

The mechanical properties of aerogel 2 were studied using compression strength measurement. During the experiments, the studied samples were gradually compressed at a rate of 1 mm/min, and each sample underwent five testing cycles. In the first experiment, a compression test was conducted on the sample at 10% of its height, repeated five times in a row (Figure 6a). The curves show that during the first test, the sample exhibits the

best physical and mechanical properties. In the course of further testing, the load at which the sample deforms by 10% decreases from 2145 Pa to 1772 Pa by the fifth test. After each cycle, the aerogel relaxes to its initial dimensions. In the case of deformation tests at 20% (Figure 6b), partial destruction of the aerogel occurs in the very first experiment at a load of 2746 Pa. However, after removing the load, the material also returns to its initial dimensions (Figure 7). In subsequent tests, the aerogel demonstrates a significant decrease in physical and mechanical characteristics, as the stress required for 10% deformation decreases from 2653 Pa to 376 Pa. Nevertheless, this still allows the aerogel to regain its shape after removing the load. Based on Figure 6b, the calculated modulus of elasticity for the original sample is 44 kPa.

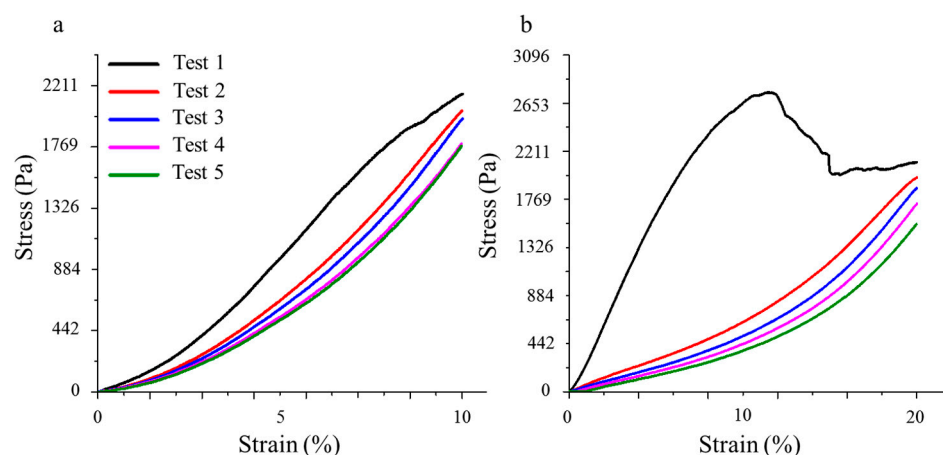


**Figure 7.** Stress–strain curves for sample compression by 10% (a) and 20% (b).

#### 4. Conclusions

We developed a novel approach to the synthesis of aerogel-like materials via a one-pot process including surfactant-free synthesis of microcapsules from partially PEGylated hyperbranched polymethylethoxysiloxane and subsequent cross-linking of microcapsules with the residual hyperbranched polymer, yielding porous bulk material. Due to the highly diphilic nature of the PEGylated PMEOS, it readily concentrates at the oil/water interface in aqueous emulsions encapsulating oil droplets. During the subsequent condensation, the organosilicon precursor is consumed for oil encapsulation (yielding hollow microcapsules) followed by the formation of a continuous porous condensed phase. Concurrently, methyl groups ensure the hydrophobicity of the resulting gels, which eliminates the need of using additional reagents for their hydrophobization. Obtained aerogels have low density (down to 0.015 g/cm<sup>3</sup>), decent specific surface area (up to 337 m<sup>2</sup>/g), while mechanical properties may be deemed satisfactory as they allow maintaining the shape and undergo some elastic deformation up to 12%.

**Author Contributions:** Conceptualization, K.B., A.B., A.K. and A.M.; methodology, K.B. and A.M.; investigation K.B.; writing—original draft preparation, K.B., A.B., A.K. and A.M.; writing—review and editing K.B., A.B., A.K. and A.M. All authors have read and agreed to the published version of the manuscript.

**Funding:** This research was funded by Russian Science Foundation, grant number 22-43-04439.

**Institutional Review Board Statement:** Not applicable.

**Informed Consent Statement:** Not applicable.

**Data Availability Statement:** The original data reported in this study are available from the corresponding author on reasonable request.

**Acknowledgments:** GPC and <sup>1</sup>H NMR analyses of PMEOS and PMEOS-PEG were carried out with the support of the Ministry of Science and Higher Education of the Russian Federation using scientific

equipment of the Center for Collective Use “Polymer Research Center” of Enikolopov Institute of Synthetic Polymeric Materials, Russian Academy of Sciences (FFSM-2021-0004).

**Conflicts of Interest:** The authors declare no conflict of interest.

## References

1. John, F.T.; Conroy, B.H. Microscale Thermal Relaxation during Acoustic Propagation in Aerogel and Other Porous Media. *Microscale Thermophys. Eng.* **1999**, *3*, 199–215. [[CrossRef](#)]
2. Forest, L.; Gibiat, V.; Woignier, T. Biot’s Theory of Acoustic Propagation in Porous Media Applied to Aerogels and Alkogels. *J. Non. Cryst. Solids* **1998**, *225*, 287–292. [[CrossRef](#)]
3. Smith, D.M.; Maskara, A.; Boes, U. Aerogel-Based Thermal Insulation. *J. Non. Cryst. Solids* **1998**, *225*, 254–259. [[CrossRef](#)]
4. Wiener, M.; Reichenauer, G.; Braxmeier, S.; Hemberger, F.; Ebert, H.-P. Carbon Aerogel-Based High-Temperature Thermal Insulation. *Int. J. Thermophys.* **2009**, *30*, 1372–1385. [[CrossRef](#)]
5. Buzykaev, A.R.; Danilyuk, A.F.; Ganzhur, S.F.; Kravchenko, E.A.; Onuchin, A.P. Measurement of Optical Parameters of Aerogel. *Nucl. Instruments Methods Phys. Res. Sect. A Accel. Spectrometers Detect. Assoc. Equip.* **1999**, *433*, 396–400. [[CrossRef](#)]
6. Jensen, K.I.; Schultz, J.M.; Kristiansen, F.H. Development of Windows Based on Highly Insulating Aerogel Glazings. *J. Non. Cryst. Solids* **2004**, *350*, 351–357. [[CrossRef](#)]
7. Dhua, S.; Gupta, A.K.; Mishra, P. Aerogel: Functional Emerging Material for Potential Application in Food: A Review. *Food Bioprocess Technol.* **2022**, *15*, 2396–2421. [[CrossRef](#)]
8. Lv, P.; Tan, X.-W.; Yu, K.-H.; Zheng, R.-L.; Zheng, J.-J.; Wei, W. Super-Elastic Graphene/Carbon Nanotube Aerogel: A Novel Thermal Interface Material with Highly Thermal Transport Properties. *Carbon N. Y.* **2016**, *99*, 222–228. [[CrossRef](#)]
9. Bryning, M.B.; Milkie, D.E.; Islam, M.F.; Hough, L.A.; Kikkawa, J.M.; Yodh, A.G. Carbon Nanotube Aerogels. *Adv. Mater.* **2007**, *19*, 661–664. [[CrossRef](#)]
10. De Marco, M.; Markoulidis, F.; Menzel, R.; Bawaked, S.M.; Mokhtar, M.; Al-Thabaiti, S.A.; Basahel, S.N.; Shaffer, M.S.P. Cross-Linked Single-Walled Carbon Nanotube Aerogel Electrodes via Reductive Coupling Chemistry. *J. Mater. Chem. A* **2016**, *4*, 5385–5389. [[CrossRef](#)]
11. Hees, T.; Zhong, F.; Rudolph, T.; Walther, A.; Mülhaupt, R. Nanocellulose Aerogels for Supporting Iron Catalysts and In Situ Formation of Polyethylene Nanocomposites. *Adv. Funct. Mater.* **2017**, *27*, 1605586. [[CrossRef](#)]
12. Li, J.; Zuo, K.; Wu, W.; Xu, Z.; Yi, Y.; Jing, Y.; Dai, H.; Fang, G. Shape Memory Aerogels from Nanocellulose and Polyethyleneimine as a Novel Adsorbent for Removal of Cu(II) and Pb(II). *Carbohydr. Polym.* **2018**, *196*, 376–384. [[CrossRef](#)]
13. Deuber, F.; Mousavi, S.; Federer, L.; Hofer, M.; Adlhart, C. Exploration of Ultralight Nanofiber Aerogels as Particle Filters: Capacity and Efficiency. *ACS Appl. Mater. Interfaces* **2018**, *10*, 9069–9076. [[CrossRef](#)] [[PubMed](#)]
14. Selmer, I.; Kleemann, C.; Kulozik, U.; Heinrich, S.; Smirnova, I. Development of Egg White Protein Aerogels as New Matrix Material for Microencapsulation in Food. *J. Supercrit. Fluids* **2015**, *106*, 42–49. [[CrossRef](#)]
15. Falahati, M.T.; Ghoreishi, S.M. Preparation of Balangu (*Lallemantia Royleana*) Seed Mucilage Aerogels Loaded with Paracetamol: Evaluation of Drug Loading via Response Surface Methodology. *J. Supercrit. Fluids* **2019**, *150*, 1–10. [[CrossRef](#)]
16. Comin, L.M.; Temelli, F.; Saldaña, M.D.A. Barley Beta-Glucan Aerogels via Supercritical CO<sub>2</sub> Drying. *Food Res. Int.* **2012**, *48*, 442–448. [[CrossRef](#)]
17. Comin, L.M.; Temelli, F.; Saldaña, M.D.A. Flax Mucilage and Barley Beta-Glucan Aerogels Obtained Using Supercritical Carbon Dioxide: Application as Flax Lignan Carriers. *Innov. Food Sci. Emerg. Technol.* **2015**, *28*, 40–46. [[CrossRef](#)]
18. Kistler, S.S. Coherent Expanded Aerogels and Jellies. *Nature* **1931**, *127*, 741. [[CrossRef](#)]
19. Yokogawa, H.; Yokoyama, M. Hydrophobic Silica Aerogels. *J. Non. Cryst. Solids* **1995**, *186*, 23–29. [[CrossRef](#)]
20. Di Luigi, M.; Guo, Z.; An, L.; Armstrong, J.N.; Zhou, C.; Ren, S. Manufacturing Silica Aerogel and Cryogel through Ambient Pressure and Freeze Drying. *RSC Adv.* **2022**, *12*, 21213–21222. [[CrossRef](#)]
21. He, X.; Tang, B.; Cheng, X.; Zhang, Y.; Huang, L. Preparation of the Methyltriethoxysilane Based Aerogel Monolith with an Ultra-Low Density and Excellent Mechanical Properties by Ambient Pressure Drying. *J. Colloid Interface Sci.* **2021**, *600*, 764–774. [[CrossRef](#)]
22. Wang, L.; Feng, J.; Jiang, Y.; Li, L.; Feng, J. Elastic Methyltrimethoxysilane Based Silica Aerogels Reinforced with Polyvinyl-methyl-dimethoxysilane. *RSC Adv.* **2019**, *9*, 10948–10957. [[CrossRef](#)]
23. Venkateswara Rao, A.; Bhagat, S.D.; Hirashima, H.; Pajonk, G.M. Synthesis of Flexible Silica Aerogels Using Methyltrimethoxysilane (MTMS) Precursor. *J. Colloid Interface Sci.* **2006**, *300*, 279–285. [[CrossRef](#)]
24. Kanamori, K.; Aizawa, M.; Nakanishi, K.; Hanada, T. New Transparent Methylsilsesquioxane Aerogels and Xerogels with Improved Mechanical Properties. *Adv. Mater.* **2007**, *19*, 1589–1593. [[CrossRef](#)]
25. Yu, Z.; Yang, N.; Apostolopoulou-Kalkavoura, V.; Qin, B.; Ma, Z.; Xing, W.; Qiao, C.; Bergström, L.; Antonietti, M.; Yu, S. Fire-Retardant and Thermally Insulating Phenolic-Silica Aerogels. *Angew. Chem. Int. Ed.* **2018**, *57*, 4538–4542. [[CrossRef](#)]
26. Kholodkov, D.N.; Arzumanyan, A.V.; Novikov, R.A.; Kashin, A.S.; Polezhaev, A.V.; Vasil’ev, V.G.; Muzafarov, A.M. Silica-Based Aerogels with Tunable Properties: The Highly Efficient BF<sub>3</sub>-Catalyzed Preparation and Look inside Their Structure. *Macromolecules* **2021**, *54*, 1961–1975. [[CrossRef](#)]

27. Zhou, B.; Shen, J.; Wu, Y.; Wu, G.; Ni, X. Hydrophobic Silica Aerogels Derived from Polyethoxydisiloxane and Perfluoroalkylsilane. *Mater. Sci. Eng. C* **2007**, *27*, 1291–1294. [[CrossRef](#)]
28. Smith, D.M.; Scherer, G.W.; Anderson, J.M. Shrinkage during Drying of Silica Gel. *J. Non. Cryst. Solids* **1995**, *188*, 191–206. [[CrossRef](#)]
29. Bhagat, S.D.; Oh, C.-S.; Kim, Y.-H.; Ahn, Y.-S.; Yeo, J.-G. Methyltrimethoxysilane Based Monolithic Silica Aerogels via Ambient Pressure Drying. *Microporous Mesoporous Mater.* **2007**, *100*, 350–355. [[CrossRef](#)]
30. Júlio, M. de F.; Ilharco, L.M. Hydrophobic Granular Silica-Based Aerogels Obtained from Ambient Pressure Monoliths. *Materialia* **2020**, *9*, 100527. [[CrossRef](#)]
31. Garrido, R.; Silvestre, J.D.; Flores-Colen, I.; de Júlio, M.F.; Pedroso, M. Economic Assessment of the Production of Subcritically Dried Silica-Based Aerogels. *J. Non. Cryst. Solids* **2019**, *516*, 26–34. [[CrossRef](#)]
32. Zhou, T.; Cheng, X.; Pan, Y.; Li, C.; Gong, L.; Zhang, H. Mechanical Performance and Thermal Stability of Glass Fiber Reinforced Silica Aerogel Composites Based on Co-Precursor Method by Freeze Drying. *Appl. Surf. Sci.* **2018**, *437*, 321–328. [[CrossRef](#)]
33. Zhai, S.; Yu, K.; Meng, C.; Wang, H.; Fu, J. Eco-Friendly Approach for Preparation of Hybrid Silica Aerogel via Freeze Drying Method. *J. Mater. Sci.* **2022**, *57*, 7491–7502. [[CrossRef](#)]
34. Güler, Ö.; Selen, V.; Başgöz, Ö.; Safa, H.; Yahia, I.S. Adsorption Properties and Synthesis of Silica Aerogel-Hollow Silica Microsphere Hybrid (Sandwich) Structure. *J. Sol-Gel Sci. Technol.* **2021**, *100*, 74–88. [[CrossRef](#)]
35. Ding, J.; Liu, Q.; Zhang, B.; Ye, F.; Gao, Y. Preparation and Characterization of Hollow Glass Microsphere Ceramics and Silica Aerogel/Hollow Glass Microsphere Ceramics Having Low Density and Low Thermal Conductivity. *J. Alloys Compd.* **2020**, *831*, 154737. [[CrossRef](#)]
36. Grandcolas, M.; Jasinski, E.; Gao, T.; Jelle, B.P. Preparation of Low Density Organosilica Monoliths Containing Hollow Silica Nanospheres as Thermal Insulation Materials. *Mater. Lett.* **2019**, *250*, 151–154. [[CrossRef](#)]
37. Kazakova, V.V.; Myakushev, V.D.; Strelkova, T.V.; Gvazava, N.G.; Muzafarov, A.M. Synthesis of Superbranched Ethylsilicates—Inorganic Dendritic Systems. *Dokl. Akad. Nauk* **1996**, *349*, 486–489.
38. Kazakova, V.V.; Rebrov, E.A.; Myakushev, V.B.; Strelkova, T.V.; Ozerin, A.N.; Ozerina, L.A.; Chenskaya, T.B.; Sheiko, S.S.; Sharipov, E.Y.; Muzafarov, A.M. From a Hyperbranched Polyethoxysiloxane Toward Molecular Forms of Silica: A Polymer-Based Approach to the Monitoring of Silica Properties. In *Silicones and Silicone-Modified Materials ACS Symposium Book Series 729*; American Chemical Society: Washington, DC, USA, 2000; Volume 729, pp. 503–515.
39. Jaumann, M.; Rebrov, E.A.; Kazakova, V.V.; Muzafarov, A.M.; Goedel, W.A.; Moller, M. Hyperbranched Polyalkoxysiloxanes via AB(3)-Type Monomers. *Macromol. Chem. Phys.* **2003**, *204*, 1014–1026. [[CrossRef](#)]
40. Chen, Z.; Zhao, Y.; Zhu, X.; Möller, M. Formation of Monodisperse Polymer@SiO<sub>2</sub> Core-Shell Nanoparticles via Polymerization in Emulsions Stabilized by Amphiphilic Silica Precursor Polymers: HLB Dictates the Reaction Mechanism and Particle Size. *Macromolecules* **2019**, *52*, 5670–5678. [[CrossRef](#)]
41. Chen, Z.; Zhao, Y.; Zhu, X. Inclusion of Hydrophobic Liquids in Silica Aerogel Microparticles in an Aqueous Process: Microencapsulation and Extra Pore Creation. *ACS Appl. Mater. Interfaces* **2021**, *13*, 12230–12240. [[CrossRef](#)]
42. Meshkov, I.B.; Kalinina, A.A.; Kazakova, V.V.; Demchenko, A.I. Densely Cross-Linked Polysiloxane Nanogels. *Ineos Open* **2020**, *3*, 118–132. [[CrossRef](#)]
43. Malkin, A.Y.; Polyakova, M.Y.; Subbotin, A.V.; Meshkov, I.B.; Bystrova, A.V.; Kulichikhin, V.G.; Muzafarov, A.M. Molecular Liquids Formed by Nanoparticles. *J. Mol. Liq.* **2019**, *286*, 110852. [[CrossRef](#)]
44. Migulin, D.; Tatarinova, E.; Meshkov, I.; Cherkaev, G.; Vasilenko, N.; Buzin, M.; Muzafarov, A. Synthesis of the First Hyperbranched Polyorganoethoxysiloxanes and Their Chemical Transformations to Functional Core-Shell Nanogel Systems. *Polym. Int.* **2016**, *65*, 72–83. [[CrossRef](#)]

**Disclaimer/Publisher’s Note:** The statements, opinions and data contained in all publications are solely those of the individual author(s) and contributor(s) and not of MDPI and/or the editor(s). MDPI and/or the editor(s) disclaim responsibility for any injury to people or property resulting from any ideas, methods, instructions or products referred to in the content.